Precise QCD Predictions for Higgs Production at the LHC

Daniel de Florian

Citation: AIP Conference Proceedings **917**, 293 (2007); doi: 10.1063/1.2751969
View online: http://dx.doi.org/10.1063/1.2751969
View Table of Contents: http://scitation.aip.org/content/aip/proceeding/aipcp/917?ver=pdfcov
Published by the AIP Publishing

Precise QCD Predictions for Higgs Production at the LHC

Daniel de Florian

Dpto. de Física, FCEyN-UBA, Buenos Aires, Argentina

Abstract. The status of QCD corrections to Higgs boson production in hadronic colliders is summarized. Results are presented for the transverse momentum distribution at the LHC including the resummation of the dominating logarithmic contributions to all orders in the coupling constant.

HIGGS PRODUCTION AND QCD

The search for the Higgs boson is among the highest priorities of the LHC physics program [1]. A significant amount of work has been devoted not only to build and design new accelerators and detectors but also to refining the necessary theoretical predictions for the various Higgs production channels and the corresponding backgrounds.

Actually during the last decades, there has been an impressive improvement in perturbative QCD calculations. Several observables have been computed to next-to-leading order (NLO) accuracy and, forced by the precision achieved by the experiments, a great effort is being performed in order to reach the same status at one order higher, NNLO.

For Higgs production, a full NNLO calculation is very complicated since it means counting, among other things, with a two-loop contribution on top of the heavy-quark loop coupling to the Higgs at the lowest order. Nevertheless, a great simplification can be achieved in the large-M_t approximation (M_t being the mass of the top quark), where the effective Lagrangian

$$\mathscr{L}_{ggH} = -\frac{H}{4v} C(\alpha_s) G^a_{\mu\nu} G_a^{\mu\nu} \tag{1}$$

involving only a gluon-gluon-Higgs vertex, as depicted in Figure 1 can be introduced. The LO cross section factors out the dependence on the top mass and the Wilson

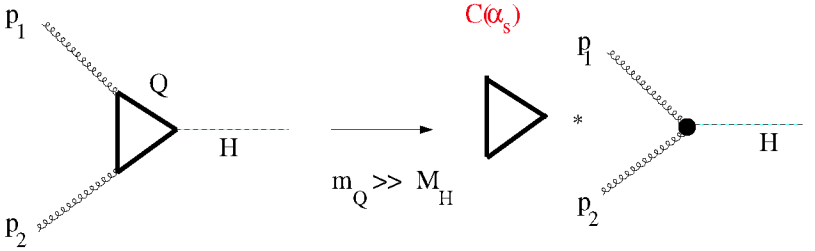

FIGURE 1. Hgg vertex in the large-M_t approximation

coefficient $C(\alpha_s)$ is known up to α_s^5 [3, 4].

CP917, *Particles and Fields,* edited by H. Castilla Valdez, J. C. D'Olivo, and M. A. Perez

While the approximation is in principle expected to be accurate only for low Higgs masses, it has been found excellent to compute the *relative* contribution of the higher order QCD corrections, within a few percent. Within this approach, NNLO results for Higgs boson production in hadronic colliders have been obtained first for the total rate [5], and more recently for fully exclusive distributions [6]. Higher order contributions are found to be quite large for the total cross-section, with NLO corrections as large as the Born contribution and a non-negligible but more moderate increase at the NNLO level. For less inclusive observables, like the transverse momentum distribution, the size of the corrections can be drastically large, at the point of completely spoiling the perturbative expansion.

This is actually a general feature in perturbative QCD: for some observables, at least under certain extreme kinematical conditions, fixed order expansions in the strong coupling constant α_s are bounded to fail. In order to have a reasonably convergent series, not only the coupling constant should be small, but also the higher order coefficients should be of $\mathcal{O}(1)$. A problem related to the last condition usually occurs in processes involving two or more energy scales at the boundaries of the phase space, where the scales take very different values. Typically a fixed order expansion for a cross section $\sigma = \left(\mathscr{C}_0 + \mathscr{C}_1 \alpha_s + \mathscr{C}_2 \alpha_s^2 + ...\right)$ depends on coefficients which contain terms proportional to logarithms of the energies involved $\mathscr{C}_n \simeq \log^m \frac{E_1}{E_2}$ with $m \leq 2n-1$.

When $E_1 \sim E_2 \gg \Lambda$ the coefficient is not affected by the presence of the logs ($\mathscr{C}_n \sim \mathcal{O}(1)$) and, at the same time, the coupling constant (evaluated at any of the scales) is small enough such that the pQCD series can converge.

On the other hand, if one of the scales is much smaller than the other, the large logs in the coefficients can spoil the convergence of the expansion no matter how small α_s is, since the power of the logarithms grows twice as fast as the power of the coupling constant. The origin of these large logarithmic contributions is well known; they arise due to an non-complete cancellation of infrared singularities between real and virtual contributions due to restrictions in the emission of particles in the boundaries of phase space. The appearance of double logs is just related to the fact that the singularities can arise due to both collinear and soft gluon radiation.

Typical examples of processes affected by such a problem are the threshold region for inclusive processes, like Drell-Yan, Higgs and event shape observables in e^+e^- and the production of high mass systems with small transverse momentum in hadronic collisions. As an example of the serious consequences of the appearance of large logarithmic contributions, we show in Figure 2 the LO and NLO transverse momentum distributions of the Higgs boson with $M_H = 125$ GeV at the LHC. While at small q_T the LO cross section increases without limit, diverging to $+\infty$, the NLO becomes negative pointing to $-\infty$, showing that the fixed order expansion makes no-sense at all at small transverse momentum.

In order to allow for a precise QCD description for such a process, the large logarithms should be *resummed* to all orders in α_S. The situation is depicted in Table 1. There, a fixed order calculation corresponds to adding all possible terms corresponding to a given *file*, i.e. to a fix power of the coupling constant. When the logarithm involved in the process is large, say when $\alpha_S \log \sim 1$, each term in a file below the one considered can be larger by a factor of $\log \sim 1/\alpha_S$ than the one evaluated at the previous order,

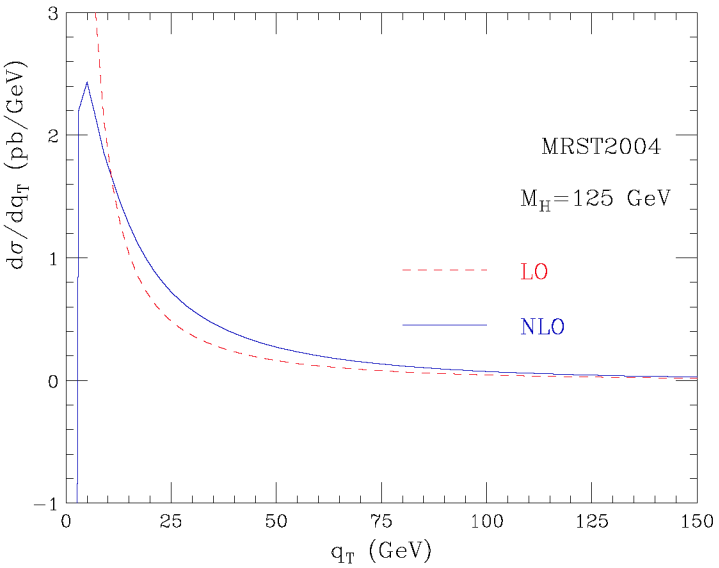

FIGURE 2. LO and NLO Higgs q_T distribution

TABLE 1. Structure of fixed order and resummed contributions

$\alpha_S \log$	.			$\mathcal{O}(\alpha_S)$ LO
$\alpha_S^2 \log^3$	$\alpha_S^2 \log^2$	$\alpha_S^2 \log$	.	$\mathcal{O}(\alpha_S^2)$ NLO
.	.	.	. .	.
.	.	.	. .	.
$\alpha_S^n \log^{2n-1}$	$\alpha_S^n \log^{2n-2}$	.	. .	$\mathcal{O}(\alpha_S^n)N...LO$
.	.	.	. .	.
.	.	.	. .	.
LL	NLL	NNLL	... ...	

even though they seem to be formally α_S suppressed! On the other hand, if all terms in a given *column* are added, the next column to the right contains terms that are actually $1/\log \sim \alpha_S$ suppressed, allowing to define a convergent expansion (if those terms can be summed to all orders).

The *resummation* can be formally achieved for a certain type of observables by showing that the large logarithms exponentiate in a Sudakov form factor such that the cross section can be written as $\sigma \sim C(\alpha_S) \exp\{\mathcal{G}(\alpha_S, \log)\}\ \sigma_{born}$ plus non-logarithmic contributions.

The Sudakov exponent is then organized according to its logarithmic accuracy; at leading-logarithmic accuracy(LL) only the highest power of the logarithm is included ($\alpha_S^n \log^{n+1}$). The second tower of logarithms in the Sudakov exponent $\alpha_S^n \log^n$ are taken into account at next-to-leading-logarithmic accuracy (NLL) and so on.

Since the resummation is relevant in the region where the logarithms are large and, on

the other hand, the fixed order expansion is valid in the opposite kinematical region, it is convenient to match both predictions in order to count with the most general description of a given observable. The matching has to be done in a consistent way in order to avoid double counting. This is achieved by defining the matched cross-section as

$$\sigma^{match} = \sigma^{res} + \sigma^{f.o.(\alpha_s^n)} - \sigma^{res}_{f.o.(\alpha_s^n)} \tag{2}$$

i.e., adding the fixed order and resummed cross-section and subtracting the fixed order expansion of the resummed contribution, which has the same small q_T limit as the fixed order contribution, therefore rendering a finite matched cross-section.

TRANSVERSE MOMENTUM DISTRIBUTIONS

An example were the resummation of the large logarithms is mandatory corresponds to the production of a Higgs boson with small transverse momentum, where the scales are the transverse momentum q_T and the mass of the Higgs M_H.

In this contribution we focus on the dominant SM Higgs production channel, gluon–gluon fusion. When the transverse momentum q_T of the Higgs boson is of the order of its mass M_H, the perturbative series is controlled by a small expansion parameter, $\alpha_S(M_H^2)$, and the fixed order prediction is reliable. The leading order (LO) calculation [7] shows that the large-M_t approximation works well as long as both M_H and q_T are smaller than M_t. In the framework of this approximation, the NLO QCD corrections have been computed [8, 9, 10, 6].

The small-q_T region ($q_T \ll M_H$) is the most important, because it is here where the bulk of events is expected. In this region the convergence of the fixed-order expansion is spoiled, since the coefficients of the perturbative series in $\alpha_S(M_H^2)$ are enhanced by powers of large logarithmic terms, $\ln^m(M_H^2/q_T^2)$. To obtain reliable perturbative predictions, these terms have to be systematically resummed to all orders in α_S as discussed in the previous section.

According to the QCD factorization theorem the corresponding transverse-momentum differential cross section[1] $d\hat{\sigma}_F/dq_T^2$ can be written as

$$\frac{d\sigma_F}{dq_T^2}(q_T, M, s) = \sum_{a,b} \int_0^1 dx_1 \int_0^1 dx_2 \, f_{a/h_1}(x_1, \mu_F^2) \, f_{b/h_2}(x_2, \mu_F^2) \, \frac{d\hat{\sigma}_{F\,ab}}{dq_T^2}(q_T, M, \hat{s}; \alpha_S(\mu_R^2)) \,, \tag{3}$$

where $f_{a/h}(x, \mu_F^2)$ ($a = q_f, \bar{q}_f, g$) are the parton densities of the colliding hadrons at the factorization scale μ_F, $d\hat{\sigma}_{F\,ab}/dq_T^2$ are the partonic cross sections, $\hat{s} = x_1 x_2 s$ is the partonic centre-of-mass energy, and μ_R is the renormalization scale.

To correctly enforce transverse-momentum conservation, the resummation has to be carried out in b space, where the impact parameter b is the variable conjugate to q_T. The resummed component of the partonic transverse-momentum cross section in Eq. (3) is

[1] To be precise, when the system F is not a single on-shell particle of mass M, what we denote by $d\hat{\sigma}_F/dq_T^2$ is actually the differential cross section $d\hat{\sigma}_F/dM^2 dq_T^2$.

then obtained by performing the inverse Fourier (Bessel) transformation with respect to the impact parameter b. We write

$$\frac{d\hat{\sigma}^{(\mathrm{res.})}_{F\,ab}}{dq_T^2}(q_T, M, \hat{s}; \alpha_S(\mu_R^2)) = \int \frac{d^2\mathbf{b}}{4\pi}\, e^{i\mathbf{b}\cdot q_T}\, \mathscr{W}^F_{ab}(b, M, \hat{s}; \alpha_S(\mu_R^2)) \tag{4}$$

$$= \int_0^\infty db\, \frac{b}{2}\, J_0(bq_T)\, \mathscr{W}^F_{ab}(b, M, \hat{s}; \alpha_S(\mu_R^2))\,, \tag{5}$$

where $J_0(x)$ is the 0th-order Bessel function.

The perturbative and process-dependent factor $\mathscr{W}^F_{ab}$ embodies the all-order dependence on the large logarithms $\ln M^2 b^2$ at large b, which correspond to the q_T-space terms $\ln M^2/q_T^2$ that are logarithmically enhanced at small q_T (the limit $q_T \ll M$ corresponds to $Mb \gg 1$, since b is the variable conjugate to q_T). Resummation of these large logarithms is better expressed by defining the N-moments $\mathscr{W}_N$ of $\mathscr{W}$ with respect to $z = M^2/\hat{s}$ at fixed M:

$$\mathscr{W}^F_{ab,N}(b, M; \alpha_S(\mu_R^2)) \equiv \int_0^1 dz\, z^{N-1}\, \mathscr{W}^F_{ab}(b, M, \hat{s} = M_H^2/z; \alpha_S(\mu_R^2))\,. \tag{6}$$

The logarithmic terms embodied in $\mathscr{W}^F_{ab,N}$ are due to final-state radiation of partons that are soft and/or collinear to the incoming partons. Their all-order resummation can be organized in close analogy to the cases of soft-gluon resummed calculations for hadronic event shapes in hard-scattering processes and for threshold contributions to hadronic cross sections. We write

$$\mathscr{W}^F_N(b, M; \alpha_S(\mu_R^2), \mu_R^2, \mu_F^2) = \mathscr{H}^F_N\left(M, \alpha_S(\mu_R^2); M^2/\mu_R^2, M^2/\mu_F^2, M^2/Q^2\right) \times \exp\{\mathscr{G}_N(\alpha_S(\mu_R^2), L; M^2/\mu_R^2, M^2/Q^2)\}\,, \tag{7}$$

The function $\mathscr{H}^F_N$ does not depend on the impact parameter b and, therefore, it contains all the perturbative terms that behave as constants in the limit $b \to \infty$. The function $\mathscr{G}$ includes the complete dependence on b and, in particular, it contains all the terms that order-by-order in α_S are logarithmically divergent when $b \to \infty$. This factorization between constant and logarithmic terms involves some degree of arbitrariness, since the argument of the large logarithms can always be rescaled as $\ln M^2 b^2 = \ln Q^2 b^2 + \ln M^2/Q^2$, provided that Q is independent of b and that $\ln M^2/Q^2 = \mathscr{O}(1)$ when $bM \gg 1$. To parametrize this arbitrariness, on the right-hand side of Eq. (7) we have introduced the scale Q, such that $Q \sim M$, and we have defined the large logarithmic expansion parameter, L, as

$$L \equiv \ln \frac{Q^2 b^2}{b_0^2}\,, \tag{8}$$

where the coefficient $b_0 = 2e^{-\gamma_E}$ ($\gamma_E = 0.5772\ldots$ is the Euler number) has a kinematical origin.

Finally, the Sudakov form factor is given by

$$\mathcal{G}_N(\alpha_S(\mu_R^2), L; M^2/\mu_R^2, M^2/Q^2) = -\int_{b_0^2/b^2}^{Q^2} \frac{dq^2}{q^2}\left[A(\alpha_S(q^2))\,\ln\frac{M^2}{q^2} + \widetilde{B}_N(\alpha_S(q^2))\right] , \tag{9}$$

where $A(\alpha_S)$ and $\widetilde{B}_N(\alpha_S)$ are perturbative functions

$$A(\alpha_S) = \frac{\alpha_s}{\pi}A^{(1)} + \left(\frac{\alpha_s}{\pi}\right)^2 A^{(2)} + \left(\frac{\alpha_s}{\pi}\right)^3 A^{(3)} + \sum_{n=4}^{\infty}\left(\frac{\alpha_S}{\pi}\right)^n A^{(n)} , \tag{10}$$

$$\widetilde{B}_N(\alpha_S) = \frac{\alpha_s}{\pi}\widetilde{B}_N^{(1)} + \left(\frac{\alpha_s}{\pi}\right)^2 \widetilde{B}_N^{(2)} + \sum_{n=3}^{\infty}\left(\frac{\alpha_S}{\pi}\right)^n \widetilde{B}_N^{(n)} . \tag{11}$$

The coefficients $A^{(n)}$ and $\widetilde{B}_N^{(n)}$, free of large logarithms, are related to the customary coefficients of the Sudakov form factors and of the parton anomalous dimensions.

In the case of the Higgs boson, the calculation of the coefficients needed to perform the resummation has been explicitly worked out at leading logarithmic (LL), next-to-leading logarithmic (NLL) [13], [14] and next-to-next-to-leading logarithmic (NNLL) [15] level.

In the following we present predictions for the Higgs boson q_T distribution at the LHC within the formalism described above. In particular, we include the most accurate description that is available at present: NNLL resummation at small q_T and NLO calculation at large q_T. An important feature of our formalism is that a unitarity constraint on the total cross section is automatically enforced, such that the integral of the spectrum reproduces the known inclusive results at NLO [17] and NNLO [5]. More details can be found in Refs. [18] and [19].

For the sake of brevity we concentrate on the quantitative results at NLL+LO (resummed+fixed order) and NNLL+NLO accuracy. At NLL+LO (NNLL+NLO)the NLL (NNLL) resummed result is matched to the LO (NLO) perturbative calculation valid at large q_T. As for the evaluation of the fixed-order results, the Monte Carlo program of Ref. [8] has been used. The numerical results are obtained by choosing $M_H = 125$ GeV and using the MRST2002 set of parton distributions [21]. At NLL+LO, LO parton densities and 1-loop α_S have been used, whereas at NNLL+NLO we use NLO parton densities and 2-loop α_S.

The NLL+LO results at the LHC are shown in Fig. 3. In the left panel, the full NLL+LO result (solid line) is compared with the LO one (dashed line) at the default scales $\mu_F = \mu_R = M_H$. We see that the LO calculation diverges to $+\infty$ as $q_T \to 0$ while the matched cross-section remains finite in the same limit. The effect of the resummation starts to be relevant below $q_T \sim 100$ GeV. In the right panel we show the NLL+LO band obtained by varying $\mu_F = \mu_R$ between $1/2M_H$ and $2M_H$.

The corresponding NNLL+NLO results are shown in Fig. 4. In the left panel, the full result (solid line) is compared with the NLO one (dashed line) at the default scales $\mu_F = \mu_R = M_H$. The NLO result diverges to $-\infty$ as $q_T \to 0$ and, at small values of q_T, it has an unphysical peak that is produced by the numerical compensation of negative leading and positive sub-leading logarithmic contributions. Notice that at $q_T \sim 50$ GeV, the q_T distribution sizably increases when going from LO to NLO and from NLO to NLL+LO.

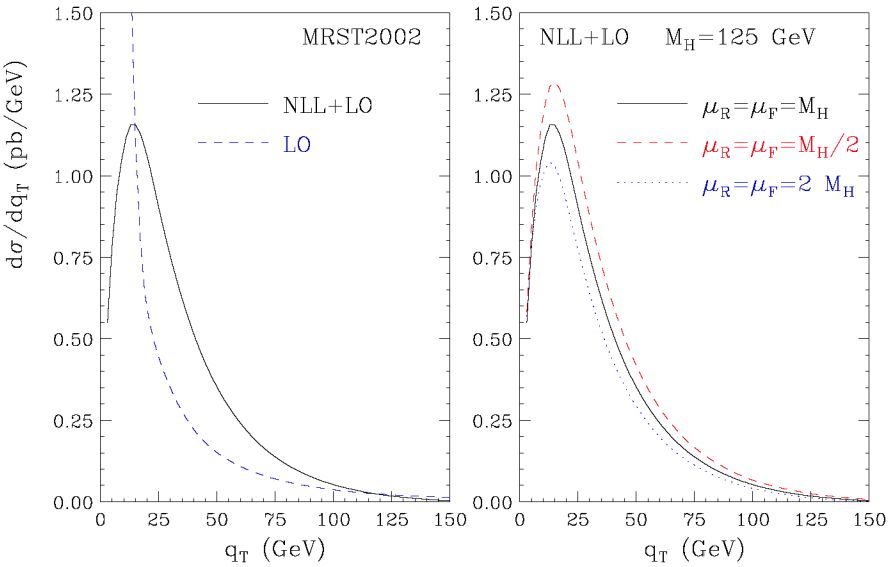

FIGURE 3. LHC results at NLL+LO accuracy.

This implies that in the intermediate-q_T region there are important contributions that have to be resummed to all orders rather than simply evaluated at the next perturbative order. The q_T distribution is (moderately) harder at NNLL+NLO than at NLL+LO accuracy while the height of the NNLL peak is a bit lower than the NLL one. This is mainly due to the fact that the total NNLO cross section (computed with NLO parton densities and 2-loop α_S), which fixes the value of the q_T integral of our resummed result, is slightly smaller than the NLO one, whereas the high-q_T tail is higher at NNLL order, thus leading to a reduction of the cross section at small q_T. The resummation effect starts to be visible below $q_T \sim 100$ GeV, and it increases the NLO result by about 40% at $q_T = 50$ GeV. The right panel of Fig. 4 shows the scale dependence computed as in Fig. 3. Comparing Figs. 3 and 4, we see that the NNLL+NLO band is smaller than the NLL+LO one and overlaps with the latter at $q_T \lesssim 100$ GeV. This suggests a good convergence of the resummed perturbative expansion allowing to reach a theoretical accuracy of the order of 10% for Higgs boson production at the LHC.

REFERENCES

1. CMS Coll., *Technical Proposal*, report CERN/LHCC/94-38 (1994); ATLAS Coll., *ATLAS Detector and Physics Performance: Technical Design Report*, Vol. 2, report CERN/LHCC/99-15 (1999).
2. *The Higgs Working Group: Summary Report*, to appear in the Proceedings of the Workshop on Physics at TeV Colliders, Les Houches, France, 2003, hep-ph/0406152.
3. Y. Schroder and M. Steinhauser, JHEP **0601**, 051 (2006).
4. K. G. Chetyrkin, J. H. Kuhn and C. Sturm, Nucl. Phys. B **744**, 121 (2006).
5. S. Catani, D. de Florian and M. Grazzini, JHEP **0105** (2001) 025; R. V. Harlander and W. B. Kilgore, Phys. Rev. D **64** (2001) 013015, Phys. Rev. Lett. **88** (2002) 201801; C. Anastasiou and K. Melnikov,

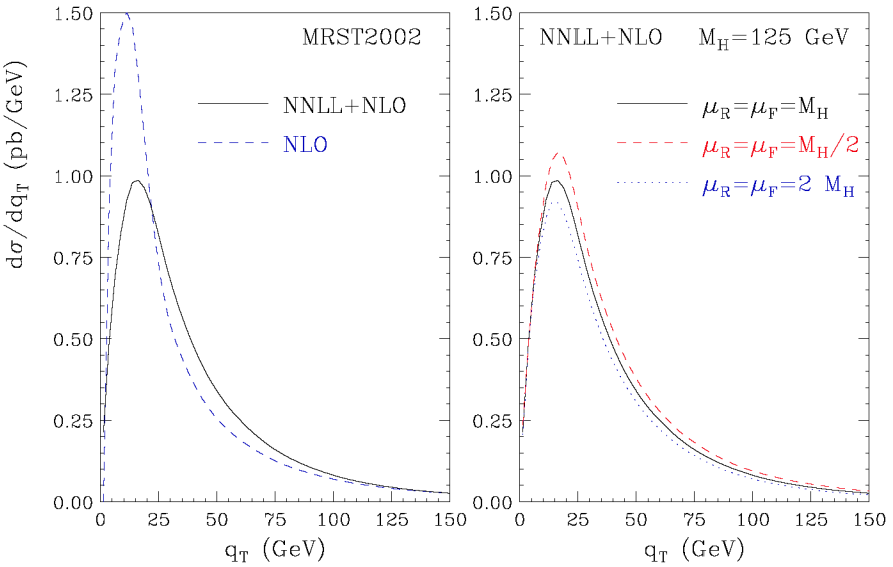

FIGURE 4. LHC results at NNLL+NLO accuracy.

Nucl. Phys. B **646** (2002) 220; V. Ravindran, J. Smith, W. L. van Neerven, Nucl. Phys. B **665** (2003) 325.

6. C. Anastasiou, K. Melnikov and F. Petriello, Phys. Rev. Lett. **93**, 262002 (2004); Nucl. Phys. B **724**, 197 (2005); S. Catani and M. Grazzini, arXiv:hep-ph/0703012.
7. R. K. Ellis, I. Hinchliffe, M. Soldate and J. J. van der Bij, Nucl. Phys. B **297** (1988) 221; U. Baur and E. W. Glover, Nucl. Phys. B **339** (1990) 38.
8. D. de Florian, M. Grazzini and Z. Kunszt, Phys. Rev. Lett. **82** (1999) 5209.
9. V. Ravindran, J. Smith and W. L. Van Neerven, Nucl. Phys. B **634** (2002) 247.
10. C. J. Glosser and C. R. Schmidt, JHEP **0212** (2002) 016.
11. G. Parisi and R. Petronzio, Nucl. Phys. B **154** (1979) 427; Y. L. Dokshitzer, D. Diakonov and S. I. Troian, Phys. Rep. **58** (1980) 269; J. C. Collins, D. E. Soper and G. Sterman, Nucl. Phys. B **250** (1985) 199.
12. S. Catani et al., hep-ph/0005025, in the Proceedings of the CERN Workshop on *Standard Model Physics (and more) at the LHC*, eds. G. Altarelli and M.L. Mangano (CERN 2000-04, Geneva, 2000), p. 1.
13. S. Catani, E. D'Emilio and L. Trentadue, Phys. Lett. B **211** (1988) 335.
14. R. P. Kauffman, Phys. Rev. D **45** (1992) 1512.
15. D. de Florian and M. Grazzini, Phys. Rev. Lett. **85** (2000) 4678, Nucl. Phys. B **616** (2001) 247.
16. S. Catani, D. de Florian and M. Grazzini, Nucl. Phys. B **596** (2001) 299.
17. S. Dawson, Nucl. Phys. B **359** (1991) 283; A. Djouadi, M. Spira and P. M. Zerwas, Phys. Lett. B **264** (1991) 440; M. Spira, A. Djouadi, D. Graudenz and P. M. Zerwas, Nucl. Phys. B **453** (1995) 17.
18. G. Bozzi, S. Catani, D. de Florian and M. Grazzini, Phys. Lett. B **564** (2003) 65.
19. G. Bozzi, S. Catani, D. de Florian and M. Grazzini, Nucl. Phys. B **737** (2006) 73.
20. C. Balazs and C. P. Yuan, Phys. Lett. B **478** (2000) 192; E. L. Berger and J. w. Qiu, Phys. Rev. D **67** (2003) 034026; A. Kulesza, G. Sterman, W. Vogelsang, Phys. Rev. D **69** (2004) 014012.
21. A. D. Martin, R. G. Roberts, W. J. Stirling and R. S. Thorne, Eur. Phys. J. C **28** (2003) 455.